

Evaluation of concrete compression strength of precast beams submitted to steam curing by the Maturity Method

Avaliação da resistência à compressão do concreto em vigas pré-moldadas submetidas à cura térmica por meio do Método da Maturidade

L. D. P. PERES ^a

eng.lucianoperes@gmail.com

M. P. BARBOSA ^b

mbarbosa@dec.feis.unesp.br

R.C.A PINTO ^c

rpinto@ecv.ufsc.br

Abstract

The Maturity Method is a non-destructive test used to evaluate concrete properties at early ages according to the material temperature history. This paper presents the application of the Maturity Method concept to estimate compression strength values for precast concrete beams with I cross sections of 50 cm and 70 cm of height submitted to steam curing in a concrete precast factory. The temperature data were collected through thermocouples inserted inside of the concrete, distributed along the length and the height of the structural element. As a consequence of the thermal cycles used in the precast plant, it was noticed that the monitored beams suffered thermal gradients during the steam curing process. It was observed that the Maturity Method was able to evaluate compression strength values at the end of thermal cycles with high accuracy.

Keywords: Maturity Method; Steam curing; Activation energy; Precast concrete; Temperature.

Resumo

O Método da Maturidade é um ensaio não destrutivo utilizado para estimar as propriedades do concreto nas idades iniciais a partir do histórico de temperaturas do material. Este artigo apresenta uma aplicação dos conceitos do Método da Maturidade para estimar valores de resistência à compressão de vigas pré-moldadas com seções transversais em I de 50 cm e 70 cm de altura submetidas a ciclos térmicos realizados junto a uma empresa de pré-moldados. As variações de temperatura tanto ao longo do comprimento quanto ao longo da altura do elemento estrutural foram observadas para os ciclos térmicos durante o dia e durante a noite. Gradientes térmicos foram observados nas vigas durante a realização da cura térmica. O Método da Maturidade permite estimar valores de resistência à compressão ao final do ciclo térmico com precisão elevada.

Palavras-chave: Método da Maturidade; Cura térmica; Energia de ativação; Pré-moldados; Temperatura.

^a Departamento de Engenharia Mecânica, Universidade Estadual Paulista "Júlio de Mesquita Filho", Campus de Ilha Solteira, eng.lucianoperes@gmail.com

Av. Brasil Centro, nº 56, CEP: 15385-000, Ilha Solteira – SP, Brasil.

^b Departamento de Engenharia Civil, Universidade Estadual Paulista "Júlio de Mesquita Filho", Campus de Ilha Solteira, mbarbosa@dec.feis.unesp.br

Alameda Bahia, nº 550, CEP: 15385-000, Ilha Solteira – SP, Brasil.

^c Departamento de Engenharia Civil, Universidade Federal de Santa Catarina, UFSC rpinto@ecv.ufsc.br, Cx. Postal 476, CEP: 88040-900, Florianópolis – SC, Brasil.

1 Introduction

The evolution of precast concrete allowed the design of projects involving various architectural forms, with applications in the construction of bridges, tunnels, hydroelectric plants, control towers of airports, etc. In order to accelerate the development of compressive strength, precast plants often use early high strength cements as well as steam curing.

The Maturity Method, from the time-temperature history of the concrete submitted to steam curing, can evaluate the evolution of concrete compression strength with time. This paper presents results obtained in a precast concrete factory in which the concrete temperatures of I-beams of 50 cm and 70 cm of height were monitored during the curing thermal cycles, for application of the Maturity Method. Estimation of the development of the concrete compression strength in the precast elements submitted to steam curing at day and night periods was performed.

2 Steam curing

The application of steam curing in precast concrete plants allows the reduction of the curing time, providing fast removal of forms and transport, as well as reduction of the storage area. This curing procedure applies higher temperatures than the ambient ones, accelerating the hydration of cement reactions. The thermal cycle can be divided in four periods as illustrated by Figure 1.

The thermal cycle involves a delay period of usually between 2 to 5 hours, followed by a heating rate of 22 to 44°C/h until reaching a constant temperature between

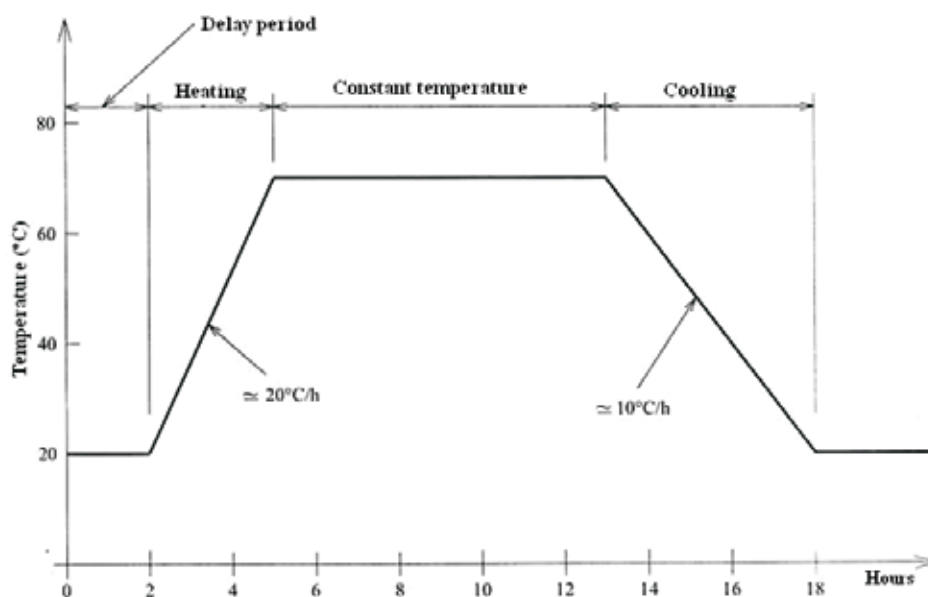
50°C and 82°C, followed by a cooling period. The total time should not surpass 18 hours (ACI [2]). During the initial stage of the hydration reactions, the temperature affects the characteristics and positioning of the products of these reactions. If the initial hydration velocity is high, there is not enough time for a proper diffusion of the products not allowing a uniform precipitation in the interstitial spaces, as in low temperatures (Verbeck e Helmuth [3]). Kanda *et al.* [4] state that at 7 days, higher strengths are obtained the higher is the temperature. However, at 28 days, there is an inversion of values. Low curing temperature provides higher final strength if compared with concrete submitted to elevated curing temperatures, They concluded that initial temperature affects the final strength of material.

In the precast plant where part of this work was accomplished, the steam curing was applied until concrete compression strength reaches 21 MPa, as measured by concrete cylinder specimens positioned near the I-beams.

3 Maturity Method

The Maturity Method was developed in England due to the need of a procedure to evaluate the effects of the temperature on strength development at different conditions of steam curing (McIntosh [5], Nurse [6], Saul [7]). Nurse [6] suggested that the product of time and temperature values was able to assess the effects of steam curing on concrete compression strength development. Saul [7] relates the maturity concept with the compression strength, in what he called the *law of gain of strength* with maturity:

Figure 1 – Thermal cycle of steam curing (El Debs (1))



“Concrete of the same mix at the same maturity (reckoned in temperature-time) has approximately the same strength, whatever combination of temperature and time go to make that maturity”.

Rastrup [8] introduced the equivalent age term - t_e , assuming that concrete reaches the same maturity index if maintained at a reference temperature until the age t_e .

Freiesleben-Hansen and Pedersen (*apud* Carino [9]), based on the Arrhenius model for the kinetics of chemical reactions (Atkins [10]), defined a mathematical function to express the maturity index in terms of equivalent ages at a reference temperature T_r , according to the Equation 1. This maturity function introduces a parameter denominated apparent activation energy (E_a), related to the thermal sensibility of the mixture.

$$t_{e(n)} = \sum_{i=1}^n e^{-\left[\frac{E_a}{R} \left(\left(\frac{1}{T_i} \right) - \left(\frac{1}{T_r} \right) \right) \right]} \cdot \Delta t_i \quad (1)$$

where:

$t_{e(n)}$ = equivalent age at reference temperature T_r (h);

E_a = apparent activation energy (J/mol);

R = universal gas constant (8.314 J/K mol);

T_a = average temperature in the time interval Δt (K);

T_r = reference temperature (K);

Δt_i = time interval (h);

3.1 Apparent activation energy

Activation energy is the difference between the energy required to trigger the reaction and the energy levels of the reactants. The term *apparent* is used to represent an average value of the activation energy of cement hydration since there are different chemical reactions happening simultaneously. Freiesleben-Hansen and Pedersen [11] suggested values of apparent activation energy related to the temperature of the concrete (T_c), in an interval of -10 °C to 80 °C:

- $T_c \geq 20$ °C: $E_a (T_c) = 33.50$ kJ/mol
- $T_c < 20$ °C: $E_a (T_c) = 33.50 + 1.47 (20 - T_c)$ kJ/mol

Carino [9] observed that most of the values is between 41 kJ/mol and 67 kJ/mol, varying according to the cementitious materials used in the concrete mixture, while ASTM C 1074-98 [12] recommends, for Type I cement, values of apparent activation energy between 40 and 45 kJ/mol, without mineral additions.

Barbosa *et al.* [13] evaluated the values of apparent activation energy for some cements manufactured in Brazil, obtaining of E_a values among 20.4 kJ/mol (CP-III-S) and 43.9 kJ/mol (CP-V-ARI), using the procedure ASTM C 1074-98 [12]. Pinto [14] presents a discussion of several experimental methods that can be used to estimate E_a in concrete mixtures.

4 Materials and experimental program

The work presented in this article was accomplished in two stages. The first one involved extensive laboratory tests necessary to determine the maturity curve and the apparent activation energy (E_a) of the concrete mixtures investigated. The second stage was performed in a precast plant where the temperature of structural elements was monitored over time during the steam curing procedure. These two stages allowed the application of the Maturity Method to estimate compression strength values of the structural elements investigated.

4.1 Elaboration of Maturity curve

The maturity curve was determined in the laboratory, for the concrete composition used by precast plant. The mixture proportions are presented in Table 1. Tables 2 and 3 show cement and aggregates characterization, respectively. The average curing temperature was 60 °C, similar to the thermal conditions used during the cycles in the precast plant.

Table 1 – Proportion of Concrete Mixture

| Materials | kg/m ³ |
|--------------------------|-------------------|
| CPV-ARI-Plus Cement | 350 |
| Water | 177 |
| Fine sand | 277 |
| Medium sand | 643 |
| Coarse aggregate (16 mm) | 1093 |

Table 2 – Physical and Chemical characterization of CP-V-ARI-Plus cement

| | | |
|-----------------------------------|---------------------------------------|-------|
| Physical Analysis | Specific surface (cm ² /g) | 4072 |
| | Apparent density (g/cm ³) | 0.94 |
| | Absolute density (g/cm ³) | 3.12 |
| | Setting time (h) | 2.12 |
| Chemical | Loss on ignition | 3.24 |
| | Insoluble residues | 0.26 |
| | SiO ₂ | 18.82 |
| | Fe ₂ O ₃ | 2.86 |
| | Al ₂ O ₃ | 5.43 |
| | CaO | 64.25 |
| | MgO | 0.89 |
| | SO ₃ | 2.75 |
| | Na ₂ O | 0.11 |
| | K ₂ O | 0.77 |
| Alkaline equiv. Na ₂ O | 0.62 | |
| Free CaO | 1.46 | |

Table 3 – Aggregate characterization

| Properties | Fine sand | Medium sand | Coarse aggregate (16 mm) |
|--|-----------|-------------|--------------------------|
| Maximum diameter (mm) | 0.595 | 2.38 | 19.0 |
| Fineness modulus | 1.39 | 2.59 | 6.51 |
| Specific mass – S.S.D.* (g/cm ³) | 2.641 | 2.622 | 2.917 |
| Specific mass – dry (g/cm ³) | 2.635 | 2.611 | 2.881 |
| Absorption (%) | 0.24 | 0.42 | 1.23 |
| Powder (%) | 0.49 | 0.05 | 0.54 |

* saturated surface dry

Several 10 x 20 cm cylinder specimens were cast and submitted to steam curing inside a designed equipment. Such equipment allowed a homogeneous distribution of the vapor produced by a boiler located close to the steam curing equipment. Heating was accomplished through electric resistances. In three specimens, evenly disposed inside the equipment, thermocouples were inserted. These thermocouples were then connected to digital multimeters for

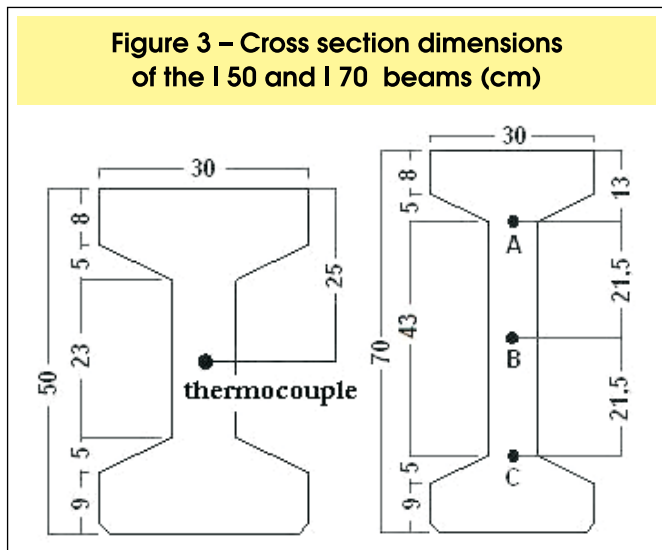
acquisition of temperature values in 5 minutes intervals during the entire thermal cycle. Type K thermocouples were used, with reading accuracy of ± 1,1 °C. Figure 2 shows the steam curing equipment.

The specimens were submitted to steam curing only after initial set time. During the thermal cycle, concrete compressive strength tests were performed at every hour. The calculation of the apparent activation energy (E_a) was de-

Figure 2 – Steam curing equipment



Figure 3 – Cross section dimensions of the I 50 and I 70 beams (cm)



terminated according to procedure ASTM C 1074-98 [12], with 5 x 5 x 5 cm mortar cubes submitted to three different curing temperatures, 30 °C, 55 °C and 80 °C.

4.2 Monitoring precast elements

In the precast plant, during casting of the structural elements, copper tubes were inserted in the concrete to facilitate the positioning of thermocouples along the height and length of the element. The thermocouples were connected to multimeters for acquisition of temperature values at every 5 minutes. The structural elements were submitted to steam curing with vapor from a boiler provisioned with wood combustion, being distributed in the inferior part of the elements. Figure 3 shows the cross sections dimensions of the monitored beams.

4.2.1 Track of the I 50 beams

Concrete temperature of I-50 beams was monitored in several sections at a 25 cm depth. At each point, a thermocouple was placed for the acquisition of temperature values. Along the track, nine sections were analyzed, according to Figure 4. Concrete specimens were also cast for compressive strength tests to be performed at every hour of the cycle. These specimens were disposed close to the track during the thermal cycle, in the points A, B

Figure 4 – Monitoring points for the track of the I 50 beams

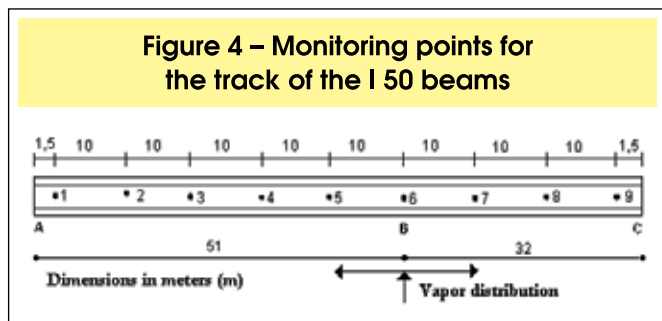
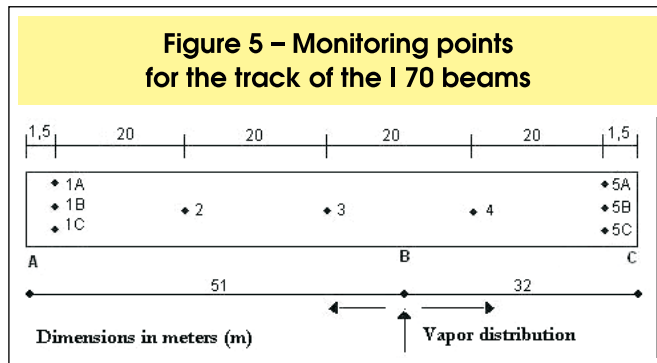


Figure 5 – Monitoring points for the track of the I 70 beams



and C. The elapsed time between the casting and the beginning of the steam curing was of 2 h.

For the track of the I 50 beams, steam curing tests were accomplished during day and night time, with the goal of evaluating the influence of the ambient temperatures on the curing processes. The same dimensions and monitoring points of temperature values were used.

4.2.2 Track of the I 70 beams

The cross section dimensions of the I 70 beams are illustrated by Figure 3. The monitoring points of temperature are disposed in Figure 5.

As well as in the track of the I 50 beams, cylindrical specimens were cast and disposed close to the track in points A, B and C. Concrete compressive strength tests were performed at every hour of the thermal cycle. The time elapsed between casting of the structural element and the beginning of the steam curing was of 3 h.

Figures 6 shows the cylinder specimens disposed close to the track of beams. Figure 7 shows a digital multimeter with thermocouple for acquisition of temperature values.

Figure 6 – Disposition of test bodies

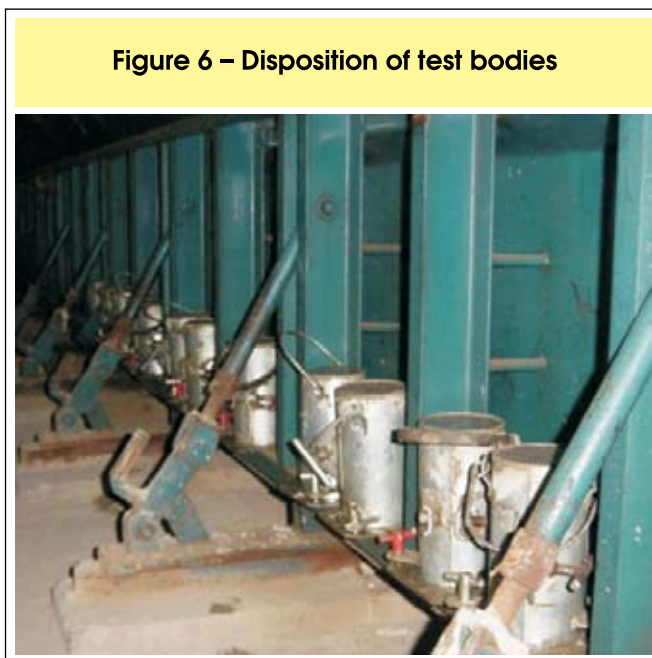
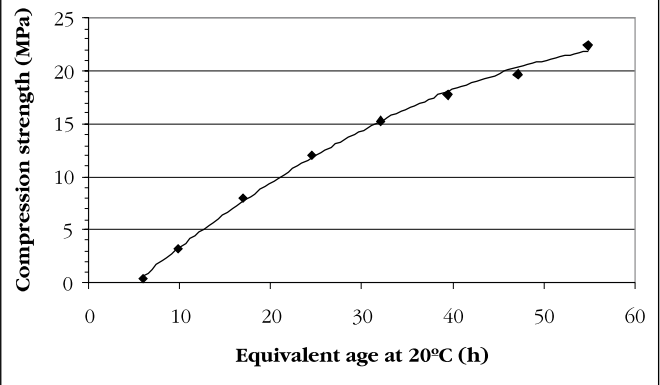


Figure 7 – Digital multimeter with thermocouple



Figure 9 – Maturity curve obtained in laboratory



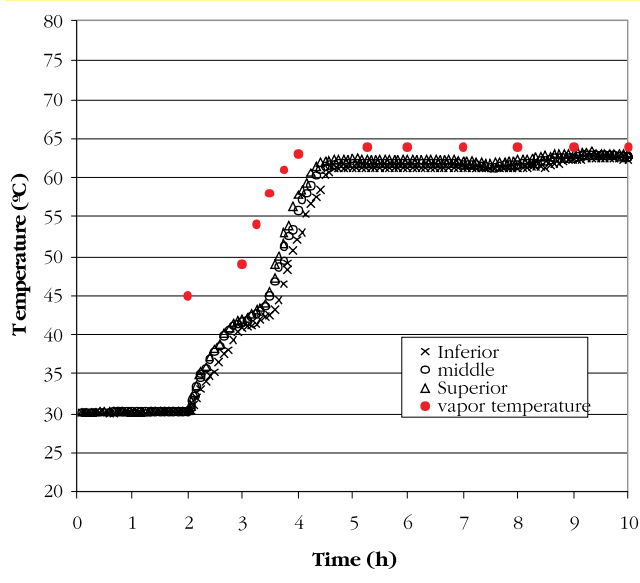
[12] procedure, and therefore used in Equation 1 to calculate the equivalent ages at every strength test.

5 Results and discussions

5.1 Maturity Curve

Figure 8 presents the development of concrete temperature inside the specimens during the thermal cycle in the laboratory, as well as the vapor temperature. The relationship between compression strength and equivalent ages at 20 °C is represented in Figure 9 for the laboratory specimens. An apparent activation energy value of

Figure 8 – Temperature versus Time (laboratory tests)



5.2 Track of the I 50 beams monitoring (day period)

Figure 10 illustrates the evolution of concrete temperatures along the track, as well as the average temperature of the vapor during heating. Casting procedures started at 3 p.m., with the application of steam curing performed at 5 p.m., with a delay period of 2 h. The ambient temperature at the beginning of the steam curing was 31 °C, decreasing until 24 °C at the end of the cycle.

Figure 10 presents all the thermal cycle stages with distinction of the delay, the heating, the constant temperature, and the cooling periods. The observed thermal gradients were of the order of 8 °C, with temperatures between 60 °C and 68 °C.

Figure 11 shows the evolution of the temperatures in the cylinder specimens disposed along the track at the points A, B and C, as indicated previously by Figure 4. The maximum temperature was around 65°C at point A, while the minimum temperature was around 58°C at point B. Such temperature range of the specimens was similar to the one observed in the beam.

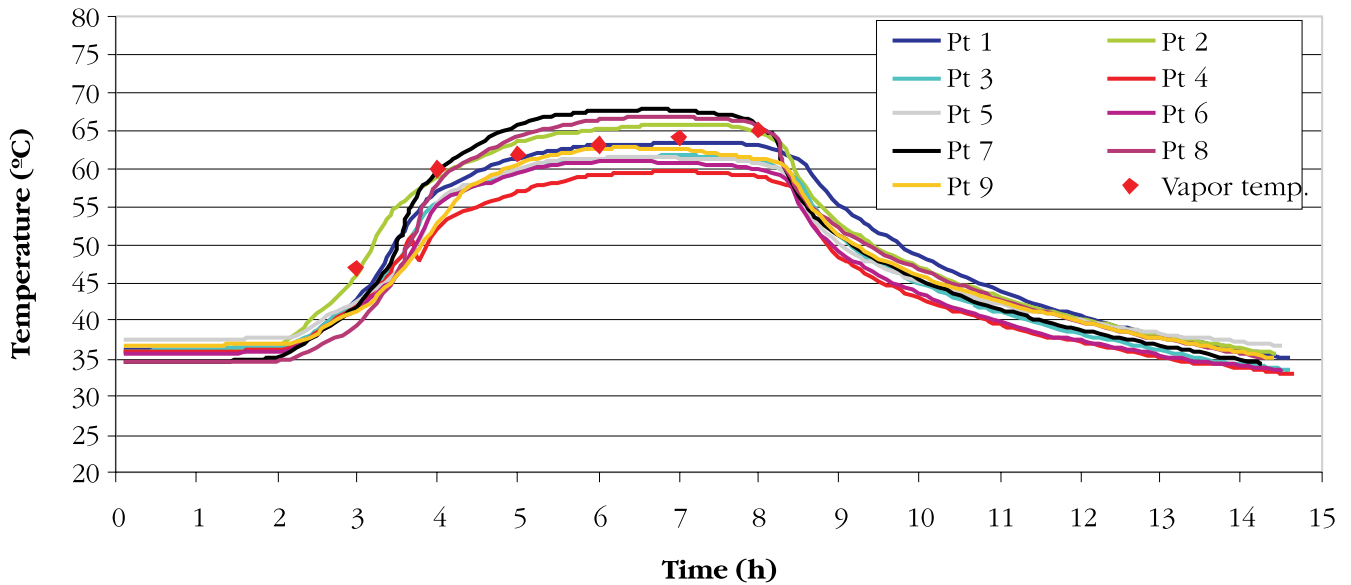
5.3 Track of the I 50 beams monitoring (night period)

Figure 12 illustrates the evolution of concrete temperatures along the track during the night period. Casting procedures started at 9 p.m., with the application of steam curing at 11 p.m., with a delay period of 2 h. The ambient temperature varied from 21.8 °C at the beginning to 18.2 °C at the end of the thermal cycle.

The thermal gradients for the I 50 beams with steam curing during the night reached values of up to 10 °C, larger than obtained values with application of the steam curing during the day. The temperature curves had a more irregular behavior when compared with the ones obtained

39.4 kJ/mol was determined from the ASTM C 1074-98

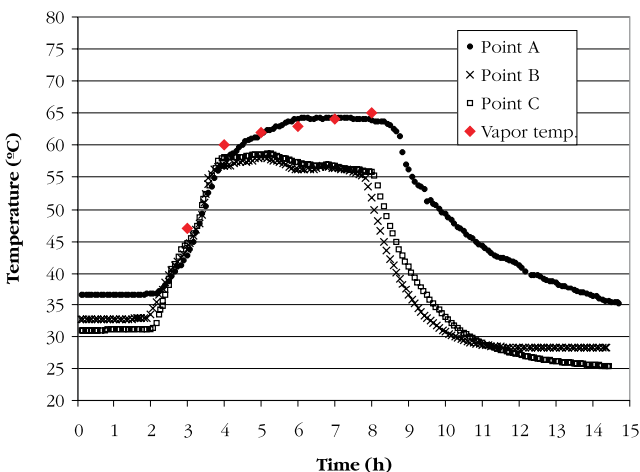
Figure 10 – Temperature versus Time for track of the I 50 beams (period of the day)



during the day period. Point 1 (at left end of the track) presented the largest temperature values, while points 8 and 9 (at right end of the track) presented the smallest temperatures.

Figure 13 illustrates the behavior of the temperature in the cylinder specimens. Temperature values were between 50 °C and 58 °C, slightly inferior to concrete temperatures in the track (55°C to 65°C). The largest temperature values were observed close to the specimens located in the extremities of the track (points A and C).

Figure 11 – Temperature versus Time for the test bodies (I 50 beams, period of the day)



5.4 Track of the I 70 beams monitoring

Casting of I 70 beams was accomplished at 3:30 p.m., with beginning of steam curing at 6:30 p.m., with a delay period equal to 3 h. The average ambient temperature was 24°C. Cylinder specimens were submitted to steam curing during 10 h until their compression strength reached 21 MPa. Figure 14 presents the temperature curves for each point analyzed during the steam curing process.

According to the Figure 14, the inferior points of the sections presented the larger temperatures due to their proximity with to the vapor exit. Temperature differences were observed along the track. Section 1 (points 1A, 1B and 1C), located in the left end, presented the smallest temperatures if compared to the ones observed in section 5 (points 5A, 5B and 5C), located in the right end of the track. Thermal gradients of the order of 20°C were observed, with temperatures between 57°C and 76°C (points 1A and 2, respectively).

The evolution of the temperature curves for the cylinder specimens is illustrated in Figure 15. The cylinders located at point C presented the largest temperatures, with maximum temperature of the order of 70°C.

5.5 Application of the Maturity Method

Compression strength values for cylinder specimens obtained during the thermal cycles in the precast plant are presented in the Table 4, as well as the theoretical values of compression strength obtained through the maturity curve elaborated in laboratory, presented in Figure 9. For the track of the I 50 beams with steam curing during the day, 10 hours of thermal cycle were

Figure 12 – Temperature versus Time for track of the I 50 beams (night period)

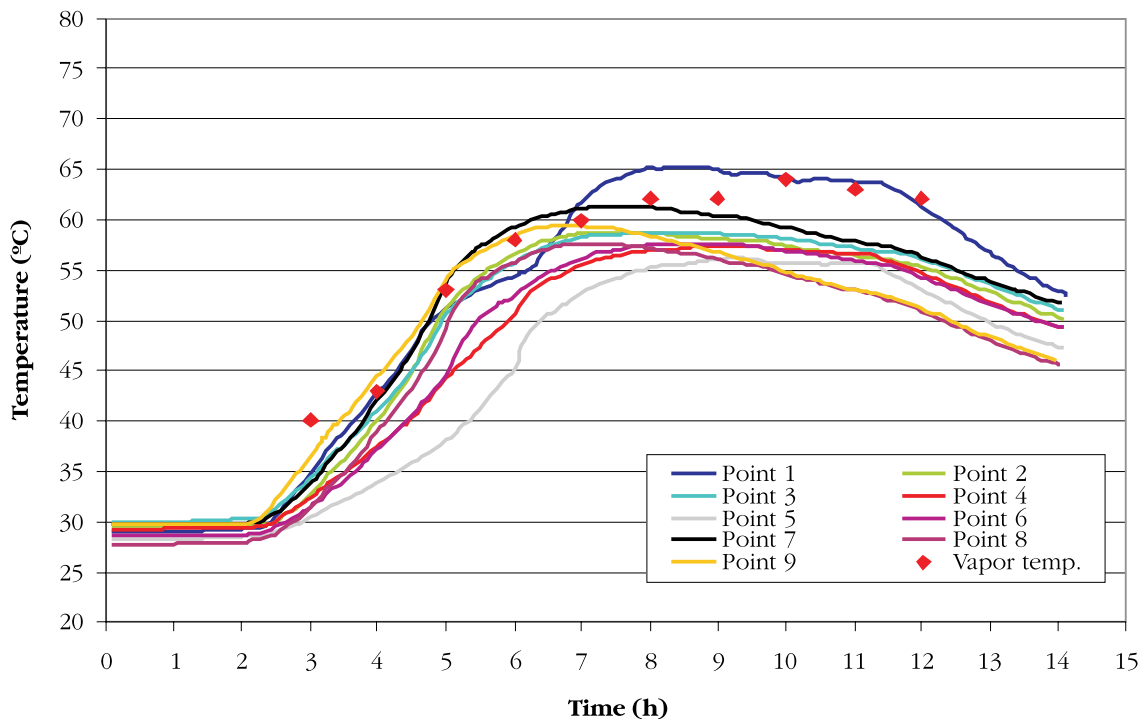


Figure 13 – Temperature versus Time for the test bodies (I 50 beams, night period)

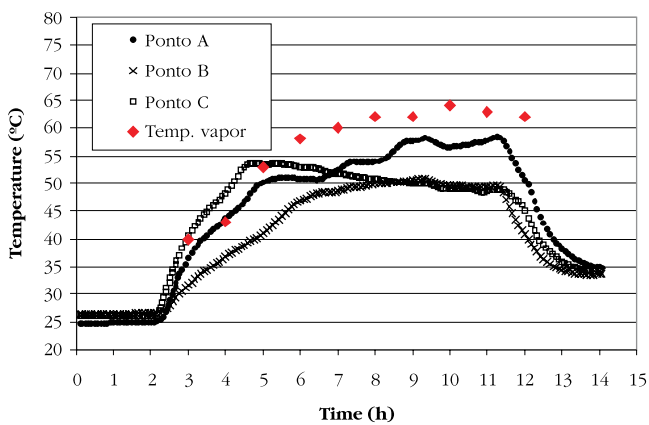


Figure 14 – Temperature versus Time for track of the I 70 beams

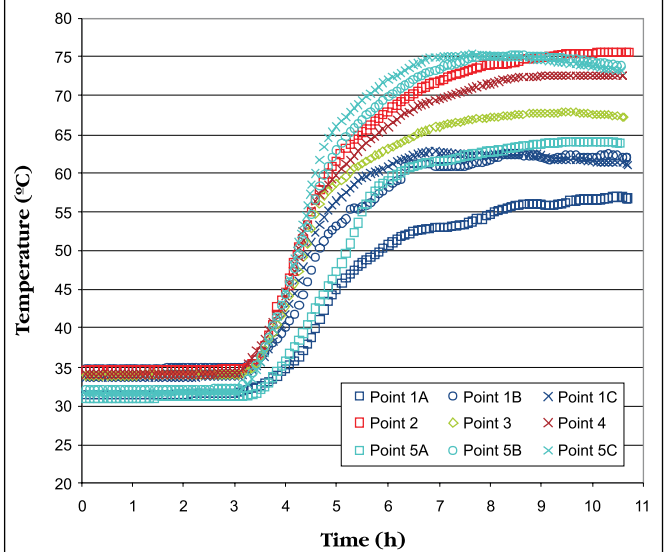
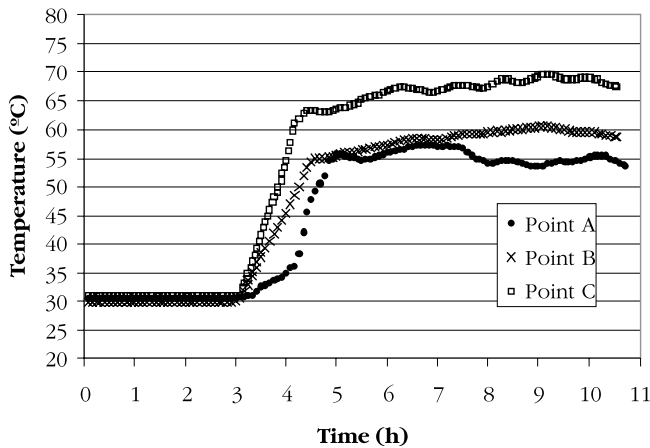


Figure 15 – Temperature versus Time for the test bodies (I 70 beams)



needed for the compression strength of cylinders reach 21 MPa, while for the cycle in the night period, 14 hours were necessary. This difference clearly indicates the influence of the ambient temperatures on the extent of the thermal cycles periods.

The error on the compression strength values of the cylinder specimens tested at the end of the thermal cycles by the maturity method was on the range of 1,1% to 11,5%. However, at the beginning of the thermal cycles, such errors were much larger, which can be explained by the small absolute values of strength at those ages.

The occurrence of thermal gradients along the track of the beams was responsible for areas with different behavior of compressive strength development. The warmest areas presented the larger strength values than the less warm areas.

Based on the obtained results, the estimation of compressive strength of the precast beams by the strength of cylinders positioned along the length of the beam is questionable. There were observed differences in strength between

Table 4 – Comparison between estimated and obtained values of compressive strength

| | Age (h) | Point A | | | | Point B | | | | Point C | | | |
|-------------------|---------|-----------|------------------|--------------------|-----------|-----------|------------------|--------------------|-----------|-----------|------------------|--------------------|-----------|
| | | t_e (h) | f_c Obt. (MPa) | f_c Estim. (MPa) | Error (%) | t_e (h) | f_c Obt. (MPa) | f_c Estim. (MPa) | Error (%) | t_e (h) | f_c Obt. (MPa) | f_c Estim. (MPa) | Error (%) |
| I 50 BEAM (DAY) | 3 | 7.4 | 0 | 1.7 | - | 6.7 | 0 | 1.1 | - | 6.3 | 0 | 0.9 | - |
| | 4 | 12.2 | 4.8 | 4.8 | 0.2 | 11.7 | 2.0 | 4.4 | 117.7 | 11.4 | 3.8 | 4.3 | 12.3 |
| | 5 | 19.2 | 8.2 | 9.0 | 9.4 | 17.9 | 6.8 | 8.2 | 21.9 | 17.9 | 8.2 | 8.2 | - |
| | 6 | 27.2 | 12.0 | 13.1 | 8.6 | 24.1 | 10.8 | 11.6 | 7.3 | 24.3 | 12.6 | 11.7 | 7.0 |
| | 7 | 35.5 | 16.7 | 16.6 | 0.5 | 30.0 | 14.8 | 14.4 | 2.8 | 30.4 | 16.6 | 14.5 | 12.3 |
| | 8 | 43.8 | 19.1 | 19.4 | 1.4 | 35.7 | 17.1 | 16.7 | 2.2 | 36.3 | 19.4 | 16.9 | 12.7 |
| | 9 | 51.3 | 20.5 | 21.2 | 3.4 | 38.9 | 19.4 | 17.8 | 7.9 | 40.4 | 20.1 | 18.3 | 8.7 |
| | 10 | 56.2 | 21.7 | 22.1 | 1.9 | 40.9 | 20.6 | 18.5 | 10.4 | 42.7 | 21.2 | 19.0 | 9.9 |
| I 50 BEAM (NIGHT) | 3 | 4.3 | 0 | 0 | - | 4.4 | 0 | 0 | - | 4.8 | 0 | 0 | - |
| | 4 | 7.3 | 0 | 1.5 | - | 6.6 | 0 | 1.0 | - | 8.4 | 0 | 2.3 | - |
| | 5 | 11.2 | 2.4 | 4.2 | 72.7 | 9.3 | 1.0 | 2.9 | 182.4 | 13.4 | 3.5 | 5.5 | 56.7 |
| | 6 | 15.9 | 7.1 | 7.1 | 0.7 | 12.7 | 3.6 | 5.1 | 43.4 | 18.6 | 7.6 | 8.6 | 13.6 |
| | 7 | 20.7 | 9.1 | 9.8 | 8.1 | 16.8 | 6.9 | 7.6 | 11.1 | 23.6 | 11.2 | 11.3 | 1.2 |
| | 8 | 26.0 | 12.1 | 12.5 | 3.3 | 21.2 | 9.9 | 10.1 | 1.9 | 28.3 | 14.5 | 13.6 | 5.8 |
| | 9 | 31.9 | 16.3 | 15.2 | 7.1 | 25.7 | 12.5 | 12.4 | 0.8 | 32.9 | 16.1 | 15.6 | 2.9 |
| | 10 | 38.1 | 17.8 | 17.6 | 1.6 | 30.3 | 15.8 | 14.5 | 8.3 | 37.3 | 17.6 | 17.3 | 1.7 |
| 14 | 55.6 | 21.3 | 22.0 | 3.4 | 42.8 | 21.0 | 19.1 | 9.2 | 50.5 | 21.3 | 21.0 | 1.1 | |
| I 70 BEAM | 4 | 7.2 | 0 | 1.5 | - | 7.7 | 0 | 1.8 | - | 8.6 | 0 | 2.5 | - |
| | 5 | 11.2 | 2.3 | 4.2 | 83.0 | 12.8 | 4.3 | 5.2 | 20.1 | 16.3 | 5.6 | 7.3 | 30.5 |
| | 6 | 16.9 | 7.9 | 7.7 | 2.9 | 18.8 | 9.4 | 8.8 | 7.2 | 25.0 | 12.0 | 12.0 | 0.3 |
| | 7 | 23.0 | 11.5 | 11.0 | 4.1 | 25.2 | 13.8 | 12.1 | 11.8 | 34.3 | 16.8 | 16.1 | 4.0 |
| | 8 | 28.8 | 14.3 | 13.8 | 3.5 | 31.9 | 15.8 | 15.2 | 3.9 | 43.8 | 19.3 | 19.4 | 0.3 |
| | 9 | 34.2 | 17.1 | 16.1 | 5.6 | 38.9 | 19.6 | 17.8 | 9.2 | 53.7 | 20.9 | 21.7 | 3.7 |
| 10 | 39.7 | 20.4 | 18.1 | 11.5 | 45.8 | 20.5 | 19.9 | 2.9 | 63.9 | 24.0 | 22.9 | 4.3 | |

the beams and the cylinder specimens, as well as, thermal gradients within the beams themselves. Therefore, cylinder strength cannot represent the beam strength accurately. Moreover, the cylinder testing can hardly describe the observed thermal gradient along the track of the beams.

The use of the maturity method, however, was able to estimate concrete compression strength values based on the temperature history of points subject to the largest solicitations or deformations, representing with better accuracy the mechanical behavior of the material when exposed to high temperatures. According to the data presented on Table 4, the maturity method estimated concrete compression strength values at the end of the thermal cycle with errors between 1.9% and 10.4% (track of the beams I 50, period of the day); 1.1% and 9.2% (track of the beams I 50, night period) and 2.9% and 11.5% (track of the beams I 70).

6 Conclusions

- For the analyzed structural elements, the application of steam curing was responsible for the appearance of temperature gradients along the length as well as in the height of the section of the beam tracks.
- Thermal differences during the curing processes resulted in strength gradients in the structure, with larger values of strength in the heated areas of the structure (extremity of the tracks).
- The ambient temperature affected the steam curing process. Considering the same acquired strength, in hot days the thermal cycles were shorter (more efficient) than in cooler days. In a cool day, there was an elevated loss of heat for the atmosphere, delaying the development of the concrete compression strength.
- In the steam curing, the vapor distribution should be accomplished in such a way to minimize thermal differences along the length and the height of the structural element, avoiding the appearance of thermal gradients in different points. As a consequence of such thermal gradients, there would be a non-homogeneous distribution of compressive strength along the length of the beam.
- Compression strength values estimated by the maturity method at the end of the thermal cycles were in the order 1.1% to 11.5% different than the actual compressive strength of cylinders. Such a small difference indicates that this non-destructive method is an important tool to be used in precast plants.
- The use of the maturity method allows the estimation of compression strength values of structural elements, being an interesting alternative in the places where it is not possible to estimate actual strength by core testing, and also where the necessary equipments to perform strength tests are not available.

7 Acknowledgements

Fundação de Amparo à Pesquisa do Estado de São Paulo (FAPESP) for its financial support;
Protendit Pré-Moldados, São José do Rio Preto – SP;

Laboratório CESP de Engenharia Civil (LCEC), Ilha Solteira – SP; and
Holcim, for the cement supply used in this work.

8 References

- [01] EL DEBS, M. K. Concreto pré-moldado: fundamentos e aplicações. São Carlos: EESC – USP, 2000. 456p.
- [02] AMERICAN CONCRETE INSTITUTE. ACI 517.2 R-87: Accelerated Curing of Concrete at Atmospheric Pressure-State of the Art. ACI Manual of Concrete, 1992.
- [03] VERBECK, G. J.; HELMUTH, R. H. Structure and physical properties of cement paste. In: INTERNATIONAL SYMPOSIUM ON THE CHEMISTRY OF CEMENT, 5, 1968, Tokyo. Proceedings... Tokyo, 1968. p. 1-32.
- [04] KANDA, T., SAKURAMOTO, F., SUZUKI, K. Compressive strength of silica fume concrete at higher temperatures. In: INTERNATIONAL CONFERENCE FLY ASH, SILICA FUME, SLAG AND NATURAL POUZZOLANS, 4, 1992, Istanbul. Proceedings... Istanbul: American Concrete Institute, 1992.
- [05] McINTOSH, J. D., Electrical Curing of Concrete. Magazine of Concrete Research, vol.1, p. 21-28, 1949.
- [06] NURSE, R. W. Steam Curing of Concrete. Magazine of Concrete Research, vol.1, nº 2, p.79-88, 1949.
- [07] SAUL, A. G. A. Principles underlying the steam curing of concrete at atmospheric pressure. Magazine of Concrete Research, vol. 2, nº 6, p. 127-140, 1951.
- [08] RASTRUP, E. Heat hydration in concrete. Magazine of Concrete Research, vol.6, nº 17, p. 79-92, 1954.
- [09] CARINO, N.J. The Maturity Method - CRC Handbook on Nondestructive Testing of Concrete. [S.l]: CRC Press, 1991. p. 101-146.
- [10] ATKINS, P.W. Physical Chemistry. 5ª edição. Melbourne: Oxford University Press, 1994. 877 p.
- [11] FREIESLEBEN-HANSEN, P.; PEDERSEN, E.J. Maturity Computer for Controlled Curing and Hardening of Concrete. Nordisk Betong, vol.1, p. 21-25, 1977.
- [12] AMERICAN STANDARD TESTING METHODS. ASTM C 1074: Practice for Estimating Concrete Strength by the Maturity Method. Filadélfia, 1998.
- [13] BARBOSA, M. P.; PINTO, R. C. A.; PERES, L. D. P. The Influence of Silica Fume on the Apparent Activation Energy of HPC Mixtures with various types of Brazilian cement. American Concrete Institute Special Publication, Farmington Hills - EUA, v. 229, p. 423-434, 2005.

- [14] Pinto, R. C. A., Determinação da Energia Aparente de Ativação da Hidratação do Cimento, e-mat – Revista de Ciência e Tecnologia de Materiais de Construção Civil. Vol. 1 nº 2, pp. 95-104, 2004.